



Pectin-Starch Biocomposite Reinforced with Rattan-Derived Cellulose Nanocrystals: A Study of Mechanical and Water Absorption Properties

Muhammad T.A. Fath^{1*}, Halimatuddahlia Nasution¹, Hamidah Harahap¹, Gina C.R. Hasibuan², Vikram Alexander¹

¹Department of Chemical Engineering, Faculty of Engineering, Universitas Sumatera Utara, Padang Bulan, Medan, 20155, Indonesia

²Department of Civil Engineering, Faculty of Engineering, Universitas Sumatera Utara, Padang Bulan, Medan, 20155, Indonesia

ARTICLE INFO

Article history:

Received 24 August 2024

Revised 05 November 2024

Accepted 13 November 2024

Published online 01 December 2024

Copyright: © 2024 Fath *et al.* This is an open-access article distributed under the terms of the [Creative Commons Attribution License](#), which permits unrestricted use, distribution, and reproduction in any medium, provided the original author and source are credited.

ABSTRACT

Bioplastics derived from natural resources such as pectin and starch often need more application due to their hygroscopic and poor mechanical properties. Employing CNC as a filler overcomes these limitations. Therefore, this study aimed to determine the effect of CNC and plasticizer contents on biocomposite based on pectin-starch. This study incorporated CNC (1, 2, 3, and 4 wt%) and glycerol (10, 20, 30, and 40 wt%) into the biocomposite formulation using the casting solution method. Characterization of the CNC was carried out using Transmission Electron Microscopy (TEM), Scanning Electron Microscopy (SEM), and Fourier Transform Infrared (FTIR). TEM and SEM analyses revealed that CNC exhibited a rod-like shape with sizes ranging from 10 to 70 nm. Based on FTIR, the CNC spectrums showed that lignin, hemicellulose, and other impurities have been removed from rattan biomass. Properties of biocomposite were analyzed using tensile, water absorption, and SEM. The suitable result of biocomposite was obtained at 2 wt% of CNC and 30 wt% of glycerol with a tensile strength of 11.18 MPa. Hence, the combination of CNC from rattan biomass and glycerol enhances the mechanical properties of the biocomposite, making it the most suitable for applications requiring improved tensile strength. At the same time, the surface morphology demonstrates improved dispersion and surface quality.

Keywords: Biocomposite, Cellulose nanocrystal, Pectin, Rattan biomass, Starch.

Introduction

Synthetic materials derived from petroleum, such as plastics, have been extensively used worldwide, but applying these materials poses significant environmental challenges. These adverse effects primarily arise from plastics' non-biodegradable nature and low thermal stability. Subsequently, renewable materials such as biopolymers can be used to reduce these challenges. Pectin is a kind of biopolymer with a high molecular weight that has already been known to be used to replace synthetic materials such as plastic due to its high biodegradability.¹ Pectin can be extracted from various waste sources, such as papaya peel, banana peel, and orange peel, offering a sustainable approach to utilizing agricultural byproducts.²⁻⁴ Pectin can be found in plant cell walls, and it is a linear chain of a methylated ester of galacturonic acid linked by a glycosidic bond (β -1,4 glycosidic). Orange peel waste is a globally abundant byproduct with high pectin contents of approximately 42.5%.⁵ Bioplastics based on biopolymers such as pectin have many advantages, such as high biodegradability, flexibility, and gelling solid ability.⁶ However, pectin-based bioplastics exhibit weak thermal stability, brittleness, poor water resistance, and low tensile strength. These weaknesses are attributed to the hydrophilic nature of pectin.⁷

In general, many strategies can be used to improve these weaknesses, such as using another natural polymer, including starch, plasticizer, and nanocrystalline cellulose as a natural filler. Combining starch and bioplastic pectin-based can improve bioplastic pectin-based physical and mechanical properties.⁸ Bioplastic based on pectin-starch still has disadvantages, such as rigidity and brittleness.^{9,10} The addition of glycerol as a plasticizer can lower the rigidity, thereby increasing the percentage elongation at the break of bioplastic based on pectin-starch.^{11,12,13}

Several natural fillers can be added to bioplastic to produce a new biocomposite product. Adding natural fillers can improve the water resistance and tensile properties of biocomposite. Natural materials such as cellulose can be obtained from abundant bioresources, including sugarcane bagasse and rattan biomass. These bioresources can be formed into cellulose nanocrystals (CNC) using chemical treatments, including sulfuric acid hydrolysis. The advantages of CNC are high interfacial area, thermal stability, tensile properties, biodegradability, and compatibility with other biopolymers.^{14,15}

The potential of CNC as a filler in biocomposites was reported based on its enhancement of mechanical properties.¹⁶ Similarly, another study showed that the addition of CNC significantly improved the tensile strength and water resistance of biocomposites.¹⁷ Previous investigations have reported using CNC in biocomposites based on pectin or starch. Therefore, the novelty of this study lies in the utilisation of CNC from rattan biomass and glycerol as biocomposite based on an orange peel pectin-starch matrix, which has yet to be reported in previous studies. This study aimed to determine the effect of CNC and glycerol contents on pectin-starch biocomposite tensile and water absorption properties. The methods used to evaluate these properties are relevant because tensile testing provides insight into the material's mechanical performance, while water absorption tests assess the bioplastic's hydrophilic behaviour, which is crucial for its potential applications in packaging and other industries. This study fills the gap by adding CNC and glycerol, which are expected to improve tensile strength and enhance water resistance. The chosen methods directly address the study objectives, allowing for a thorough evaluation of how

*Corresponding author. E mail: thorIQ@usu.ac.id
Tel: +6281360891823

Citation: Fath MTA, Nasution H, Harahap H, Hasibuan GCR, Alexander V. Pectin-Starch Biocomposite Reinforced with Rattan-Derived Cellulose Nanocrystals: A Study of Mechanical and Water Absorption Properties. Trop J Nat Prod Res. 2024; 8(11): 9138 - 9144 <https://doi.org/10.26538/tjnpr/v8i11.24>

Official Journal of Natural Product Research Group, Faculty of Pharmacy, University of Benin, Benin City, Nigeria

CNC and glycerol influence the overall performance of the pectin-starch bioplastic.

Materials and Methods

The equipment used includes a sieved tray (100 mesh, RLS Test Sieve Analysis Mart'1 S/Steel, Indonesia), analytical balance (Mettler Toledo, AB204S, Switzerland), Whatman filter paper, ultrasound (Elma S300 H, Germany), hot plate (Thermo Scientific, Cimarec, United States) and acrylic mould (handmade).

The biocomposite formulation included cellulose nanocrystals (CNC) derived from a recent investigation as a filler.¹⁴ Orange peel waste and sago starch were purchased in a Setia Budi SB—group market (3°34'15.0"N 98°38'30.8" E) in January 2018. Aquadest, analytical grade hydrochloric acid (HCl, Merck, 37%), ethanol (C₂H₅OH, Merck, 96%) and glycerol (Merck, 99%), sodium chloride (NaCl, Merck), phenolphthalein (C₂₀H₁₄O₄), sodium hydroxide (NaOH, Merck), were obtained as received.

Pectin Isolation from Orange Peel Waste

Orange peel waste was washed and dried under the sun. The dried orange peel waste was sieved to 100 meshes. About 6 g of orange peel waste was extracted using 250 mL of hydrochloric acid (HCl) at 60°C for an hour. The extracted solution was filtered, and ethanol was added until a precipitate formed. The precipitate formed was dried and sieved to 100 meshes. Pectin powder was analyzed for equivalent weight, methoxyl content, galacturonic acid content, and degree of esterification.¹⁸

Biocomposite Preparation

Biocomposite preparation was carried out according to the procedure with some modifications.⁷ About 3 g matrix with the ratio of 55 wt% of pectin and 45 wt% of starch are weighed. The amount of CNC varied from 1 - 4 wt% of the matrix was dissolved using 75 ml of aquadest. Subsequently, it was dispersed using an ultrasound for 30 minutes, and sago starch was added to the CNC-dispersed solution. The CNC-starch dispersed solution was poured into 75 ml of pectin (blended solution). Approximately 10 - 40 wt% of glycerol matrix was added to the combined solution. The solution was heated at 70°C and poured into an acrylic mould.

Pectin Characterizations

The pectin powder from the extraction process was characterised using titrimetric methods, including equivalent weight, methoxyl content, galacturonic acid content, and degree of esterification.

Morphological Analysis

The morphological observation of the biocomposite was analyzed using a scanning electron microscope (SEM, EVO MA 10, ZEISS, Germany). The morphology of CNC was analyzed by using Transmission Electron Microscopy (TEM, Philips CM30, Netherlands) and SEM.¹⁹

Fourier Transform Infrared (FTIR)

The biocomposite was subjected to FTIR analysis using Fourier Transform Infrared (FTIR, Shimadzu, IR-21, Japan) and was recorded with a wavelength range of 4000 cm⁻¹ - 500 cm⁻¹.

Tensile properties

Tensile properties, including tensile strength and elongation at break, were determined according to ASTM D882-02 by Universal Testing Machine (Instron, United States). Each measurement was replicated three times to ensure reliability.

Water Absorption

Biocomposite film was cut at 2 x 2 cm² weighed as dry weight, and placed on Petri dishes containing water. The dry film was weighed

every 20 minutes until the weight was constant. Water absorption was calculated from Eq. 1.¹⁶

$$\text{Water absorption} = \frac{\text{Wet Weight} - \text{Dry Weight}}{\text{Dry Weight}} \quad (1)$$

Statistical analysis

The data collected was further analysed using Statistical Package Software for Social Sciences (SPSS) IBM Corp., version 29.0.2.0, released 2023 for analysis of variance (ANOVA) followed posthoc by Tukey's test to express the data distribution by significant value ($p < 0.05$). Tensile strength, elongation at break, and water absorption were included in the statistical analysis.

Results and Discussion

The results of equivalent weight, methoxyl content, galacturonic acid content, and degree of esterification of pectin powder are presented in Table 1. Based on these results, pectin can be classified as low methoxyl pectin (LMP). LMP does not have the gelling forming ability, mechanical properties, or high methoxyl pectin (HMP).¹⁸ Furthermore, these weaknesses of LMP can be prevented by blending with starch.⁷ Previous studies obtained LMP from different sources, such as wild plums yielded 5.32 ± 0.2% LMP with 90°C HCl and 6.48 ± 0.1% with 45°C HCl,²⁰ lemon pomace yielded 4.24 ± 0.46% for mature fruit and 4.26 ± 0.01% for overripe fruit,²¹ and dragon fruit yielded 3.43 ± 0.31% using 0.03 M HCl.²² These comparative results suggest that the extraction method employed for orange peel pectin was effective, yielding competitive results relative to other plant-based sources of LMP. The relatively high yield of LMP from orange peel underscores its potential as a viable alternative source for pectin extraction.

Table 1: Weight loss percentage of rattan biomass and CNC

No	Characterization	Result	Standard
1.	Equivalent weight (mg)	510.52	600 – 800
2.	Methoxyl (%)	5.20	>7.12 (high methoxyl pectin)
3.	Galacturonic acid (%)	64.06	<7.12 (low methoxyl pectin)
4.	Degree of esterification (%)	46.09	60
			>50% (high ester content)
			<50% (low ester content)

The scanning electron microscope (SEM) and Transmission Electron Microscopy (TEM) analyses were performed to observe the cellulose nanocrystals (CNC) morphology and to measure the size of the CNC. Based on previous investigations, the CNC was obtained from rattan biomass using a 60% sulfuric acid concentration.¹⁴ Based on Figure 1(A), CNC shows the presence of cellulose crystallites in rod-shaped form. Subsequently, it shows that the intra-fibrillar structure, the impurities, and the amorphous region of cellulose have been successfully decomposed and disintegrated into individual crystallites.²³ The TEM analysis of CNC is shown in Figure 1(B). The morphologies show that CNC is rod-shaped with an average size of 10-70 nm and agglomerated with other formulations. The agglomerated CNC was caused by its unique characteristics such as high surface area, hydrophilic solid, and Van der Waals interactions.²⁴ The same result was reported with kenaf fibres as the raw material of CNC.¹⁷

The agglomerated CNC reduces the physical interactions between filler and matrix. However, the dispersion method using ultrasound can be used to reduce the agglomerated CNC. The smaller the CNC size as filler in the matrix, the higher the surface area and the increased adhesion, thereby enhancing the physical interaction between the filler and the matrix.²⁵

The FTIR spectrums of rattan biomass and cellulose nanocrystals (CNC) are shown in Figure 2, and the interpretation is shown in Table 2. Both spectra show a prominent peak at 3348 cm⁻¹, corresponding to the O-H stretching vibration in cellulose. The sharper absorption of the

O-H group in CNC is due to the presence of acid and alcohol groups introduced during the CNC isolation process. The C-H stretching vibration appears at 2927 cm^{-1} in both samples, indicating aliphatic hydrocarbon chains.²⁶ A significant absorption peak at 1724 cm^{-1} in rattan biomass corresponds to C=O stretching from hemicellulose and possibly lignin, which is absent in CNC, indicating the removal of lignin and hemicellulose during CNC production.²⁷ A notable peak shift is observed from 1608 cm^{-1} in rattan biomass to 1639 cm^{-1} in CNC, representing the O-H bending of adsorbed water. The sharper O-H bending peak in CNC suggests a stronger interaction between adsorbed water and the O-H groups in CNC.²⁸ This functional group is typical of cellulose and absent in other components like hemicellulose and lignin. The peaks at 1423 cm^{-1} in rattan biomass and 1472 cm^{-1} in CNC are attributed to C-H asymmetric deformation. The sharper peak in CNC indicates a higher cellulose contribution than lignin. Peaks at 1053 cm^{-1} in rattan biomass and 1004 cm^{-1} in CNC represent C-O stretching, with the sharpness of this peak in CNC confirming the presence of pyranose rings characteristic of cellulose.²⁸ Lastly, the peaks at 902 cm^{-1} in rattan biomass and 898 cm^{-1} in CNC are assigned to the β -1,4-glycosidic bond, with the sharp absorption in CNC signifying its crystalline structure.²⁹

The results of determining the tensile properties of CNC and glycerol are shown in Figure 3, which shows the effect of cellulose nanocrystals (CNC) and glycerol contents on tensile strength values. The higher the CNC and glycerol contents, the higher the tensile strength values of biocomposite until the highest value at 2 wt% for CNC and 30 wt% for glycerol (11.18 MPa) is attained. The optimum value at 2 wt% of CNC content showed that CNC has dispersed, distributed, and filled the matrix's unfilled spots.³⁰ Similar structures of CNC (filler), pectin, and starch (matrix) will create strong adhesion and hydrogen interactions between CNC and pectin-starch.^{7,31} The dispersion of CNC and the resulting strong interactions create an effective interface area, as shown in Figure 4(A). Adding 1 wt% of CNC did not show an excellent tensile strength value compared to 2, 3, and 4 wt%. This suggests that the CNC content was insufficient to fill the voids in the matrix, leading to unevenness in the wetting process. This result is also supported by the scanning electron microscope (SEM) image in Figure 4(B), where the biocomposite still has a large cavity. However, the tensile strength of biocomposite decreased at 3 and 4 wt% of CNC contents due to the agglomeration and non-uniform of CNC that reduced the interaction between filler and matrix.^{30,32} It was also supported by the SEM image in Figure 4(C), where the biocomposite showed a rough surface compared to the others. Some investigations with different matrix types, such as high methoxyl pectin and sago starch, also reported these results.^{7,16} Based on Figure 3, the tensile strength of biocomposites improved continuously with glycerol content up to 30 wt%. This enhancement is attributed to the intramolecular bonds in pectin and starch being penetrated by glycerol, which facilitates increased hydrogen bonding between pectin, starch, and CNC.³³ In Figure 5(A),

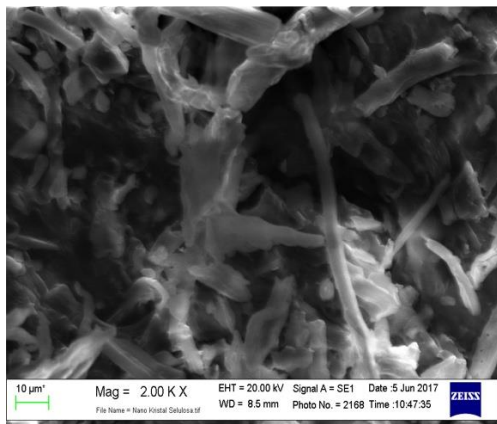
the biocomposite shows a more stable surface with no significant tortuous on the surface of the biocomposite. However, at 20 wt%, glycerol did not show an optimum value. This revealed that some pectin and starch particles have not dispersed adequately, resulting in a non-uniform biocomposite surface. Additionally, the glycerol content as a plasticizer appears insufficient to effectively reduce the solid intermolecular and intramolecular bonds in pectin and starch, forming numerous voids. This ultimately results in a less uniform stress distribution, as shown in Figure 5b.³⁴ Furthermore, the higher glycerol content at 40 wt% reduced the tensile strength of biocomposite due to the higher glycerol presence that would penetrate the intramolecular bonds in pectin and starch and the intermolecular and intramolecular bonds. The SEM image of the biocomposite with 40 wt% of glycerol content is shown in Figure 5c, which shows that the biocomposite still has some tortuousness on the surface caused by excessive glycerol content. Excessive glycerol content increases the interaction between glycerol and glycerol, producing a plastisol film.^{33,35} Figure 6 shows the effect of CNC and glycerol contents on the elongation at the break of biocomposites. The presence of CNC content decreased the elongation at the break of the biocomposite until it reached an optimum value of 2 wt% of the CNC content. CNC, when used as a filler, imparts significant stiffness, thereby enhancing the overall rigidity of biocomposite. This effect is influenced by the interactions between CNC, pectin, and starch, which lead to more restricted movement of the polymer chains. As a result, the distance between intermolecular bonds is reduced, ultimately decreasing the elongation at the break of the biocomposite.³⁰ However, it can also be seen from Figure 6 that the elongation at the break of biocomposites was enhanced by 3 and 4 wt% of CNC contents. This is because of the tendency of non-uniform and agglomeration of CNC with pectin-starch solution, which can lower the stiffness of the biocomposite.^{7,30} The lower stiffness in biocomposite results in a higher elongation at break. As shown in Figure 6, increasing glycerol content leads to higher elongation at break for the biocomposites. The maximum elongation, reaching 29%, was achieved with a glycerol content of 40% and a CNC content of 1%. This is due to the glycerol ability to penetrate the intramolecular bonds in pectin and starch. However, precisely, it would penetrate the intermolecular and intramolecular bonds and be replaced with a strong interaction between glycerol. This interaction reduces the stiffness of the biocomposite, thereby increasing its flexibility and mobility.¹ Statistical analysis using ANOVA on CNC and glycerol content on tensile strength and elongation is presented in Table 3. The results showed that the p-value was more significant than 0.05, indicating that the data was normally distributed and the effects were statistically insignificant. Previous studies reported similar findings of $p > 0.05$ for the mechanical properties of starch-based films plasticized with glycerol and lignin reinforced with cellulose nanocrystals, indicating that these properties are not significantly different.³⁶

Table 2: Interpretation of FTIR spectra of rattan biomass and cellulose nanocrystals

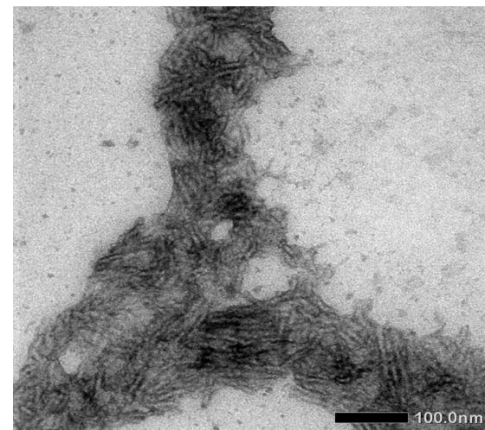
Wavenumber (cm^{-1}) Literature	Wavenumber (cm^{-1}) Experimental	Band Interaction	Band Assignment	Possible Compounds
3500–3200	3402 (Rattan biomass)	Stretch	O-H (Hydroxyl group)	Cellulose, hemicellulose, lignin
3500–3200	3348 (CNC)	Stretch	O-H (Hydroxyl group)	Cellulose
2950–2850	2927 (Rattan biomass)	Stretch	C-H (Alkyl group)	Lignin, hemicellulose
2950–2850	2897 (CNC)	Stretch	C-H (Alkyl group)	Cellulose
1750–1650	1724 (Rattan biomass)	Stretch	C=O (Carbonyl group)	Hemicellulose, lignin
1650–1600	1639 (CNC)	Bend (adsorbed water)	O-H (Hydroxyl group)	Water (adsorbed)
1650–1600	1608 (Rattan biomass)	Bend	O-H (Hydroxyl group)	Water (adsorbed), Cellulose
1500–1400	1423 (Rattan biomass)	Stretch	C-H (Methyl, methylene)	Cellulose, lignin
1500–1400	1472 (CNC)	Stretch	C-H (Methyl, methylene)	Cellulose
1100–1000	1053 (Rattan biomass)	Stretch	C-O (Carbohydrate region)	Cellulose, hemicellulose
1100–1000	1004 (CNC)	Stretch	C-O (Carbohydrate region)	Cellulose
900–890	902 (Rattan biomass)	Stretch	β -1,4-glycosidic link	Cellulose, hemicellulose

Table 3: Variables and results of ANOVA analysis used in this study

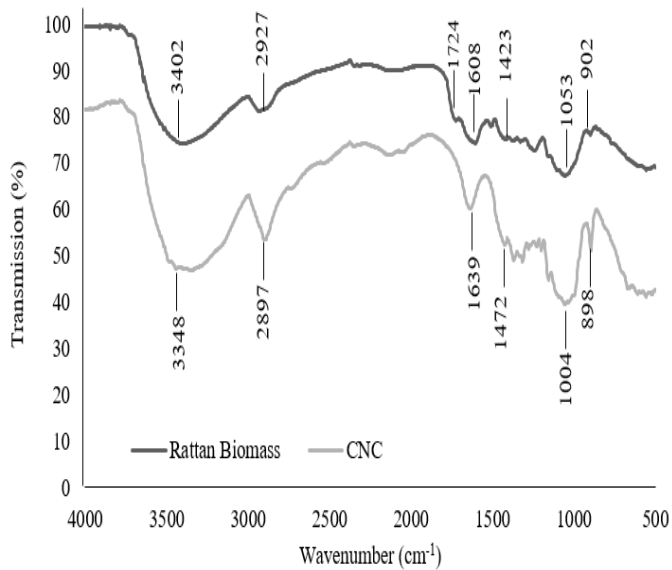
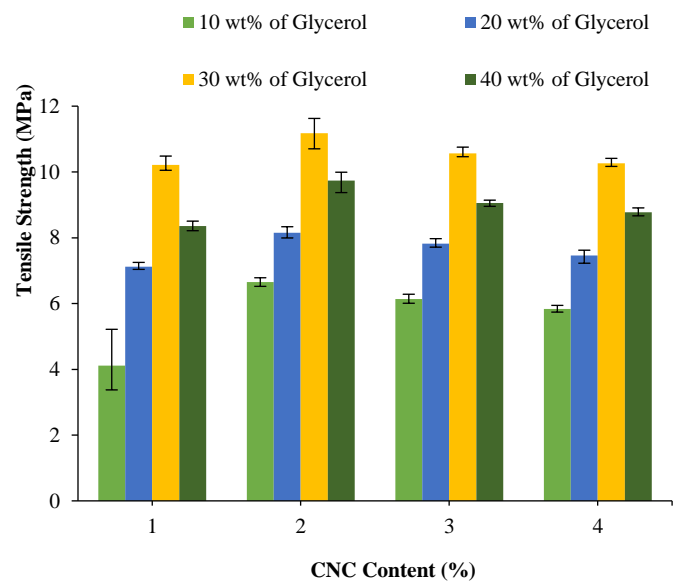
Variables	Description	Sum of Squares	df	Mean Square	F	Sig.
CNC content on tensile strength	Between groups	4.554	3	1.518	0.347	0.792
	Within groups	52.529	12	4.377		
Glycerol on Tensile strength	Between groups	51.277	3	17.092	3.532	0.289
	Within groups	5.807	12	0.484		
CNC content on elongation	Between groups	44.188	3	14.729	0.605	0.624
	Within groups	292.250	12	24.354		
Glycerol on elongation	Between groups	284.688	3	94.896	2.205	0.239
	Within groups	51.750	12	4.313		
CNC content on water absorption at 30 wt% of glycerol content	Between groups	131.108	3	43.703	0.954	0.428
	Within groups	1282.145	28	45.791		
Time on water absorption at 30 wt% of glycerol content	Between groups	1249.897	7	178.557	2.623	0.314
	Within groups	163.356	24	6.806		
Glycerol content on water absorption at 2 wt% of CNC content	Between groups	70.324	3	23.441	0.856	0.475
	Within groups	766.346	28	27.369		
Time on water absorption at 2 wt% of CNC content	Between groups	751.761	7	107.394	3.035	0.195
	Within groups	84.909	24	3.538		



a



b

Figure 1: CNC morphology of a) SEM analysis on 2000x magnification and b) TEM analysis on 100 nm magnification**Figure 2:** FTIR analysis of rattan biomass and CNC**Figure 3:** The effect of CNC and glycerol contents on the tensile strength of biocomposites

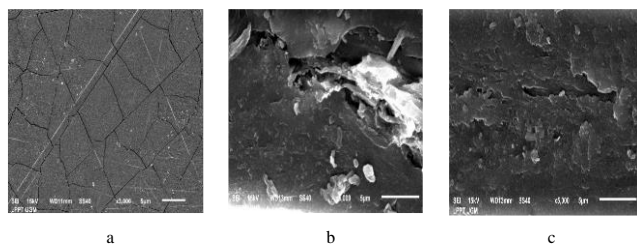


Figure 4: Morphology of (A) Biocomposite filled with 2 wt% of CNC and 30 wt% of glycerol contents on 3000x magnification, (B) Biocomposite filled with 1 wt% of CNC and 30 wt% of glycerol contents on 5000x magnification and (C) Biocomposite filled with 4 wt% of CNC and 30 wt% of glycerol on 5000x magnification

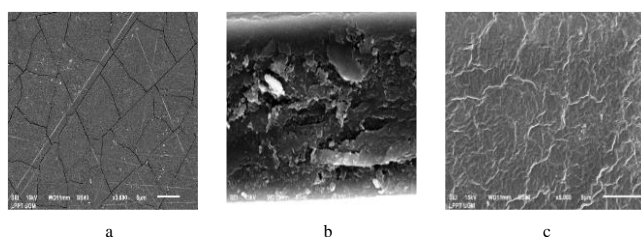


Figure 5: Morphology of (A) Biocomposite filled with 2 wt% of CNC and 30 wt% of glycerol contents on 3000x magnification, (B) Biocomposite filled with 2 wt% of CNC and 20 wt% of glycerol contents on 5000x magnification and (C) Biocomposite filled with 2 wt% of CNC and 40 wt% of glycerol contents on 5000x magnification

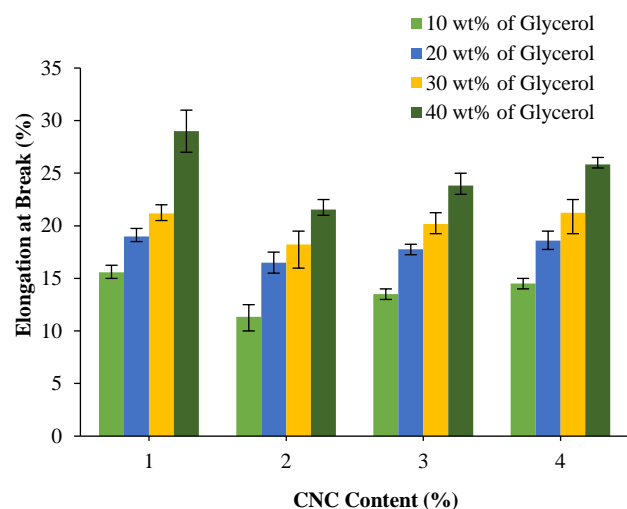


Figure 6: The effect of CNC and glycerol contents on the elongation at break of biocomposites

Figure 7 shows the effect of cellulose nanocrystals (CNC) content on the water absorption of biocomposites at 30 wt% of glycerol content. The figure shows that the addition of CNCs at 30 wt% of glycerol content obtained a constant time of water absorption properties at the 140th minute with the value of biocomposites at 1, 2, 3, and 4 wt% of CNC were 19.44, 15.79, 20.40 and 21.81% respectively. The figure shows a significant increase in water absorption of all biocomposites, specifically in the first 20 minutes. The first 20 minutes of immersion showed that CNC had a high capacity for water absorption, facilitating easier water penetration into biocomposites. Furthermore, it shows that the water absorption of biocomposites remained constant at the 60th minute. This is due to the decreased ability of CNC to absorb water until reaching a saturation point of water absorption. As observed,

biocomposite with 2 wt% CNC content represents the optimal value for water absorption. This can be attributed to the crystalline structure, the smaller size of the CNC, and the physical interactions between CNC and pectin-starch, which enhance the density of the biocomposite. On the other hand, the higher the density of biocomposite, the better water resistance biocomposite results will be produced.³⁷ However, at 3 and 4 wt% of CNC contents, the water absorption of biocomposites increased due to the agglomeration of CNC and the existence of an amorphous region in CNC, which makes water more accessible to diffuse to biocomposite, increasing its water absorption properties. Similarly, Figure 8 shows the effect of glycerol content on water absorption at 2 wt% of CNC content. At the 140th minute (constant time of water absorption properties), the value of biocomposites at 10, 20, 30, and 40 wt% of glycerol were 12.50, 13.79, 15.78, and 16.66%, respectively. Biocomposites absorbed water rapidly during the initial 20 minutes of immersion, reaching saturation by the 60th minute. From Figure 8, it can be observed that the higher the glycerol content, the higher the water absorption of biocomposites. This occurred due to the hydrophilic properties of glycerol that might make the bonds brittle when exposed to water.³⁸ This result was also supported by the scanning electron microscope (SEM) image in Figure 5(C), where the higher plasticizer content produced a plastisol film. Glycerol tends to interact more with plastic film, increasing biocomposite water absorption. Statistical analysis using ANOVA on CNC content and time on water absorption at 30 wt% of glycerol content and glycerol content and time on water absorption at 2 wt% of CNC content is presented in Table 3. The results showed a p-value >0.05, indicating that the data was normally distributed and the effects were statistically insignificant. Previous studies found similar p > 0.05 for the water absorption of starch and chitosan nanocomposite films, indicating no statistically significant differences in the results.³⁹

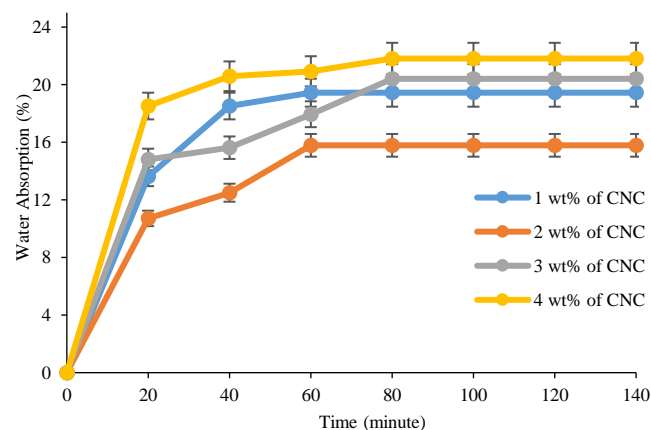


Figure 7: The CNC content effect on the biocomposites water absorption at 30 wt% of glycerol content

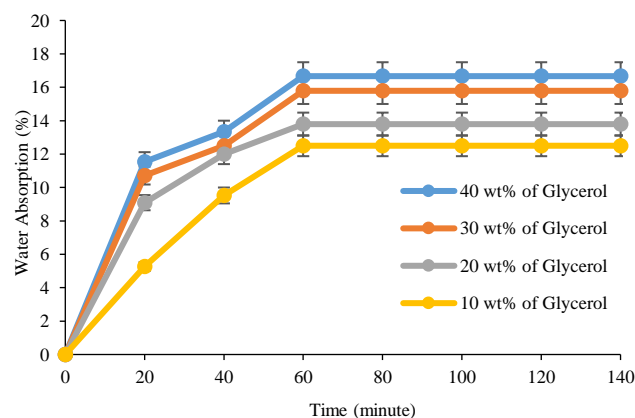


Figure 8: The effect of glycerol content on water absorption at 2 wt% of CNC content

Conclusion

Morphological analysis showed that sulphuric acid hydrolysis resulted in single cellulose nanocrystals (CNC) crystallites with a dimension of approximately 10 – 70 nm. The removal of hemicellulose, lignin, and other compounds in CNC was shown by Fourier Transform Infrared (FTIR) analysis. The suitable result of biocomposite was obtained at 2 wt% of CNC and 30 wt% of glycerol with a tensile strength of 11.18 MPa. Future studies could investigate alternative plasticizers or surface treatments that enhance the hydrophobicity of the biocomposite, making it more suitable for moisture-sensitive applications like packaging.

Conflict of Interest

The authors declare no conflict of interest.

Authors' Declaration

The authors hereby declare that the work presented in this article is original and that any liability for claims relating to the content of this article will be borne by them.

References

- Jantrawut P, Chaiwarit T, Jantanasakulwong K, Brachais CH, Chambin O. Effect of plasticizer type on tensile property and *in vitro* indomethacin release of thin films based on low-methoxyl pectin. *Polymers*. 2017;9(289):1-14. Doi: 10.3390/polym9070289
- Mada T, Duraisamy R, Guesh F. Optimization and characterization of pectin extracted from banana and papaya mixed peels using response surface methodology. *Food Sci Nutr*. 2022;10(4):1222–1238. Doi: 10.1002/fsn3.2754
- Swamy GJ, Muthukumarappan K. Optimization of continuous and intermittent microwave extraction of pectin from banana peels. *Food Chem*. 2017;220:108–114. Doi: 10.1016/j.foodchem.2016.09.197
- Bátori V, Jabbari M, Ákesson D, Lennartsson PR, Taherzadeh MJ, Zamani A. Production of Pectin-Cellulose Biofilms: A New Approach for Citrus Waste Recycling. *Int J Polym Sci*. 2017;9732329:1-9. Doi: 10.1155/2017/9732329
- Fath MT Al, Nasution H, Harahap H, Ayu GE. Biocomposite of pectin and starch-filled with nanocrystalline cellulose (NCC): The effect of filler loading and glycerol addition. *AIP Conf Proc*. 2019;2175(020012):1-7. Doi: 10.1063/1.5134576
- Mellinas C, Ramos M, Jiménez A, Garrigós MC. Recent trends in the use of pectin from agro-waste residues as a natural-based biopolymer for food packaging applications. *Materials (Basel)*. 2020;13(3):1-17. Doi: 10.3390/ma13030673
- Chaichi M, Hashemi M, Badii F, Mohammadi A. Preparation and characterization of a novel bionanocomposite edible film based on pectin and crystalline nanocellulose. *Carbohydr Polym*. 2017;157:167–175. Doi: 10.1016/j.carbpol.2016.09.062
- Arooj A, Khan M, Munawar KS. Preparation and physicochemical characterization of starch/pectin and chitosan blend bioplastic films as future food packaging materials. *J Environ Chem Eng*. 2024;12(111825):1-8. Doi: 10.1016/j.jece.2023.111825
- Al Fath MT, Ayu GE, Hasibuan GCR, Dalimunthe NF, Alexander V. The Effect of Glycerol and Sago Starch Addition on the Characteristics of Bioplastics Based on Orange Peel Pectin. *Chem Ind Chem Eng Q*. 2024;30(4):359–365. Doi: 10.2298/CICEQ231214007A
- Dompo SI, Tanor MN, Rahardiyani D, Gedoan SP, Moko EM. Effect of Acid Modification on the Physico-Chemical Properties of North Sulawesi's Giant Swamp Taro (GST) Starch (*Cyrtosperma merkusii*). *Trop J Nat Prod Res*. 2024;8(1):5869–5874. Doi: 10.26538/tjnpr/v8i1.23
- Fath MTA, Ayu GE, Lubis M, Hasibuan GCR, Dalimunthe NF. Mechanical And Thermal Properties Of Starch Avocado Seed Bioplastic Filled With Cellulose Nanocrystal (CNC) As Filler And Potassium Chloride (KCl) As Dispersion Agent. *Rasayan J Chem*. 2023;16(3):1630–1636. Doi: 10.31788/RJC.2023.1638464
- Nasution H, Harahap H, Al Fath MT, Afandy Y. Physical properties of sago starch biocomposite filled with Nanocrystalline Cellulose (NCC) from rattan biomass: The effect of filler loading and co-plasticizer addition. *IOP Conf Ser Mater Sci Eng*. 2018;309(1):1–6. Doi: 10.1088/1757-899X/309/1/012033
- Farahnaky A, Saberi B, Majzoobi M. Effect of glycerol on physical and mechanical properties of wheat starch edible films. *J Texture Stud*. 2013;44(3):176–186. Doi: 10.1111/jtxs.12007
- Fath M, Nasution H. Process optimization of manufacturing nanocrystalline cellulose from rattan biomass using sulfuric acid. *AIP Conf. Proc.* 2018;020020:1-6. Doi: 10.1063/1.5064306
- Harahap H, Hayat N, Lubis M. Preparation and application of nanocrystalline cellulose derived from sugarcane waste as filler modified alkanolamide on crosslink of natural rubber latex film. In: *AIP Conference Proceedings*. *AIP Conf. Proc.* 2017;(1865)040012:1-6. Doi: 10.1063/1.4993354
- Nasution H, Harahap H, Al Fath MT, Afandy Y. Physical properties of sago starch biocomposite filled with Nanocrystalline Cellulose (NCC) from rattan biomass: The effect of filler loading and co-plasticizer addition. *IOP Conf. Ser.: Mater. Sci. Eng.* 2018;309(01203):1-6. Doi: 10.1088/1757-899X/309/1/012033.
- Zainuddin SYZ, Ahmad I, Kargazadeh H, Abdullah I, Dufresne A. Potential of using multiscale kenaf fibres as reinforcing filler in cassava starch-kenaf biocomposites. *Carbohydr Polym*. 2013;92(2):2299–2305. Doi: 10.1016/j.carbpol.2012.11.106
- Sharma PC, Gupta A, Kaushal P. Optimization of method for extraction of pectin from apple pomace. *Indian J Nat Prod Resour (IJNPR)[Formerly Nat Prod Radiance (NPR)]*. 2015;5(2):184–189. Doi: 10.56042/ijnpr.v5i2.2182
- Perumal AB, Nambiar RB, Sellamuthu PS, Sadiku ER, Li X, He Y. Extraction of cellulose nanocrystals from areca waste and its application in eco-friendly biocomposite film. *Chemosphere*. 2022;287:1-12. Doi: 10.1016/j.chemosphere.2021.132084
- Khan M, Nandkishor. Optimization of Extraction Condition and Characterization of Low Methoxy Pectin From Wild Plum. *J Packag Technol Res*. 2019;3(3):215–221. Doi: 10.1007/s41783-019-00070-z
- Azad AKM. Isolation and Characterization of Pectin Extracted from Lemon Pomace during Ripening. *J Food Nutr Sci*. 2014;2(2):30-35. Doi: 10.11648/j.jfns.20140202.12
- Ismail NSM, Ramli N, Hani NM, Meon Z. Extraction and characterization of pectin from dragon fruit (*Hylocereus polyrhizus*) using various extraction conditions. *Sains Malaysiana*. 2012;41(1):41–45.
- Mazlita Y, Lee H V, Hamid SBA. Preparation of cellulose nanocrystals bio-polymer from agro-industrial wastes: Separation and characterization. *Polym Polym Compos*. 2016;24(9):719–728. Doi: 10.1177/09673911160240090
- Chu Y, Sun Y, Wu W, Xiao H. Dispersion properties of nanocellulose: a review. *Carbohydr Polym*. 2020;250(116892):1-17. Doi: 10.1016/j.carbpol.2020.116892
- Bilbao-Sainz C, Bras J, Williams T, Sénechal T, Orts W. HPMC reinforced with different cellulose nano-particles. *Carbohydr Polym*. 2011;86(4):1549–1557. Doi: 10.1016/j.carbpol.2011.06.060

26. Morán JI, Alvarez VA, Cyras VP, Vázquez A. Extraction of cellulose and preparation of nanocellulose from sisal fibres. *Cellulose*. 2008;15:149–159. Doi: 10.1007/s10570-007-9145-9
27. Liew FK, Hamdan S, Rahman MR, Rusop M, Lai JCH, Hossen MF, Rahman MM. Synthesis and characterization of cellulose from green bamboo by chemical treatment with mechanical process. *J Chem*. 2015;212158:1-7. Doi: 10.1155/2015/212158
28. Alemdar A, Sain M. Isolation and characterization of nanofibers from agricultural residues—Wheat straw and soy hulls. *Bioresour Technol*. 2008;99(6):1664–1671. Doi: 10.1016/j.biortech.2007.04.029
29. Karim MZ, Chowdhury ZZ, Hamid SBA, Ali ME. Statistical optimization for acid hydrolysis of microcrystalline cellulose and its physiochemical characterization by using metal ion catalyst. *Materials (Basel)*. 2014;7(10):6982–6999. Doi: 10.3390/ma7106982
30. Agustin MB, Ahmmad B, Alonzo SMM, Patriana FM. Bioplastic based on starch and cellulose nanocrystals from rice straw. *J Reinf Plast Compos*. 2014;33(24):2205–2213. Doi: 10.1177/0731684414558325
31. Rosa MF, Chiou BS, Medeiros ES, Wood DF, Williams TG, Mattoso LH, Orts WJ, Imam SH. Effect of fibre treatments on tensile and thermal properties of starch/ethylene vinyl alcohol copolymers/coir biocomposites. *Bioresour Technol*. 2009;100:5196–5202. Doi: 10.1016/j.biortech.2009.03.085
32. Francucci G, Rodríguez ES, Vázquez A. Study of saturated and unsaturated permeability in natural fibre fabrics. *Compos Part A Appl Sci Manuf*. 2010;41(1):16–21. Doi: 10.1016/j.compositesa.2009.07.012
33. Fishman ML, Coffin DR, Unruh JJ, Ly T. Pectin/starch/glycerol films: blends or composites? *J Macromol Sci Part A Pure Appl Chem*. 1996;33(5):639–654. Doi: 10.1080/10601329608010884
34. Meneguín AB, Cury BSF, Dos Santos AM, Franco DF, Barud HS, da Silva Filho EC. Resistant starch/pectin free-standing films reinforced with nanocellulose intended for colonic methotrexate release. *Carbohydr Polym*. 2017;157:1013–1023. Doi: 10.1016/j.carbpol.2016.10.062
35. Fishman ML, Coffin DR, Onwulata CI, Konstance RP. Extrusion of pectin and glycerol with various combinations of orange albedo and starch. *Carbohydr Polym*. 2004;57(4):401–413. Doi: 10.1016/j.carbpol.2004.05.014
36. Miranda CS, Ferreira MS, Magalhães MT, Santos WJ, Oliveira JC, Silva JBA, José NM. Mechanical, Thermal, and Barrier Properties of Starch-based Films Plasticized with Glycerol and Lignin and Reinforced with Cellulose Nanocrystals. *Mater Today Proc*. 2015;2(1):63–69. Doi: 10.1016/j.matpr.2015.04.009
37. Liu D, Zhong T, Chang PR, Li K, Wu Q. Starch composites reinforced by bamboo cellulosic crystals. *Bioresour Technol*. 2010;101(7):2529–2536. Doi: 10.1016/j.biortech.2009.11.058
38. Lu Y, Weng L, Cao X. Morphological, thermal and mechanical properties of ramie crystallites—reinforced plasticized starch biocomposites. *Carbohydr Polym*. 2006;63(2):198–204. Doi: 10.1016/j.carbpol.2005.08.027
39. Vieira SR, da Silva JBA, Druzian JI, de Jesus Assis D, Mussagy CU, Pereira JFB, Santos-Ebinuma VC, Lemos PVF, Correia PR, de Souza Ferreira E, de Souza CO. Cellulose Nanoparticles Prepared by Ionic Liquid-Assisted Method Improve the Properties of Bionanocomposite Films. *J Polym Environ*. 2022;30(8):3174–3185. Doi: 10.1007/s10924-022-02420-6